Nitrogen diffusion in R_2Fe_{17} lattice: a trapping diffusion process

1997 J. Phys.: Condens. Matter 9 1201

(http://iopscience.iop.org/0953-8984/9/6/007)

J. Phys.: Condens. Matter **9** (1997) 1201–1216. Printed in the UK PII: S0953-8984(97)75637-6

Nitrogen diffusion in R_2Fe_{17} lattice: a trapping diffusion process

Y D Zhang†‡§, J I Budnick†‡§, W A Hines†§, N X Shen† and J M Gromek§

† Department of Physics, University of Connecticut, Storrs, CT 06269, USA

‡ Connecticut Advanced Technology Center for Precision Manufacturing, University of Connecticut, Storrs, CT 06269, USA

§ Institute of Materials Science, University of Connecticut, Storrs, CT 06260, USA

Received 21 June 1996, in final form 24 September 1996

Abstract. X-ray diffraction, thermoconductivity and nuclear magnetic resonance experiments have been carried out in order to study the diffusion mechanism of N atoms in the Y_2Fe_{17} lattice. These experiments reveal that a small number of N atoms which enter the Y_2Fe_{17} lattice, but do not occupy the octahedral interstitial sites, are mobile at the nitrogenation temperature, while most of the N atoms, which enter the octahedral sites, are immobilized. Based on the characteristics of nitrogenation observed in R_2Fe_{17} (were R is the rare-earth element) systems, a tripping diffusion model has been proposed and discussed in detail. The previously proposed free diffusion model is the high-temperature approximation of the trapping diffusion model. The experiments and theoretical analysis show that it is the N–lattice interaction, instead of N–N interaction, that leads to the formation of the observed nitrided–unnitrided configuration, causes a tremendous decrease of the apparent diffusion frequency factor and is responsible for the N uptake stability and irreversibility. Also, this work shows how the N–lattice interaction affects the N uptake in various nitrogenation conditions.

1. Introduction

The discovery of $R_2Fe_{17}(C, N, H)_x$ (R is a rare-earth element) obtained by the gas–solid reaction approach [1–3] has attracted considerable research activity. $Sm_2Fe_{17}(C, N)_x$ (2:17) is very promising candidate as a permanent magnetic material due to its high Curie temperature and large uniaxial magnetic anisotropy. However, the phase decomposition from 2:17 into RN (RC) and α-Fe, which occurs during the nitrogenation process at temperatures above 350 °C, is a factor destructive of the permanent magnet performance. In order to optimize the nitrogenation (carbonation) conditions for inserting a large number of N or C atoms into the 2:17 lattice with a homogeneous distribution and without causing a severe phase decomposition, knowledge of the nature of the gas–solid reaction and the detailed aspects of the N uptake process is urgently needed.

N atoms enter the 2:17 lattice through a diffusion process, mostly occupying the octahedral interstitial sites. Due to the phase decomposition, the nitrogenation temperatures are restricted to be below 500 °C. Based on previous studies [4–14], the principal features of nitrogenation can be summarized as follows.

(i) N uptake is irreversible, i.e., under vacuum, the N atoms which have entered the octahedral sites cannot be pumped out within the same length of time as for nitrogenation, even when the temperature is the same [4].

0953-8984/97/061201+16$19.50

(ii) In an intermediate stage of the nitrogenation process, the N atoms absorbed in an R_2Fe_{17} particle form a two-phase (nitrided–unnitrided) configuration, i.e., the N atoms are concentrated in a nitrided region, leaving the remaining part of the particle unnitrided. The nitrogenation process is the growth of the size of the nitrided region while the N concentration in the nitrided region does not change [5–9].

(iii) For some systems, such as $Y_2Fe_{17}N_x$, the above-mentioned nitrided–unnitrided N distribution pattern formed during a nitrogenation process does not change in a vacuum annealing process at the same temperature and within about the same length of time as for nitrogenation [6]. For some systems, such as $Sm_2Fe_{17}N_x$, such steplike N distribution can be changed by annealing to reach a homogeneous N distribution, but it requires a much longer time than nitrogenation [12, 13].

(iv) For a free diffusion process, the diffusion activation energy, E_a, and diffusion constant, D, are correlated by

$$D = D_0 e^{-E_a/k_B T} \tag{1}$$

where D_0 is the diffusion frequency factor, k_B is the Boltzmann constant and T is the absolute temperature. It was found that the measured value of D_0 for N diffusion in the 2:17 phase is much smaller than the value for N diffusion in metals [4, 10].

To date, very little is known concerning the N diffusion mechanism. In the initial attempt to treat the N diffusion process, it was assumed that all of the N atoms which enter the 2:17 lattice were mobile with the same diffusion constant, and the N distribution in the particle was described by a continuous solid solution (see [10] and [11]; this is referred to as the free diffusion model hereafter). However, some experimental results cannot be explained by the free diffusion model [5–9], and the nitrogenation is more like a trapping diffusion process [14].

Whether the octahedral-site nitrogen atoms are trapped or are free to migrate, and how the nitrogenation process evolves, are fundamental issues in understanding the nitrogenation process. These issues are also intimately related to the optimization of the nitrogenation conditions. In this work, we use x-ray diffraction (XRD), thermoconductivity detection (TCD) and nuclear magnetic resonance (NMR) experiments to explore the diffusion behaviour of N atoms and the nitrogenation mechanism in the Y_2Fe_{17} lattice. Since the experimental results reveal the immobilization of the octahedral-site N atoms, we extend the diffusion equation to a trapping diffusion process, i.e., to a system containing two types of interstitial atom subject to different interactions with the lattice and, hence, having different diffusivities. A comparison between the solutions of trapping diffusion equations and the experimental results shows that the above-mentioned features of nitrogenation for the 2:17 phase can be well understood based on the immobilization of N atoms after occupying the octahedral interstitial sites. It turns out that the N uptake is more like a chemical reaction diffusion process.

2. Experimental procedure and results

A parent Y_2Fe_{17} ingot was made by arc melting; powder samples with particle diameters ranging from 32 to 37 μm were selected for nitrogenation. The powder was annealed at 900 °C in an Ar atmosphere for 5 d. The $Y_2Fe_{17}N_x$ samples with $0.3 < x < 2.8$ were obtained by annealing the powder samples under an ultra-high-purity N_2 (99.999%) gas flow at 480 °C for different periods of time from 20 min to 12 h. When the oven was turned off, the temperature decreased to 300 °C in less than 15 min, below which N diffusion actually

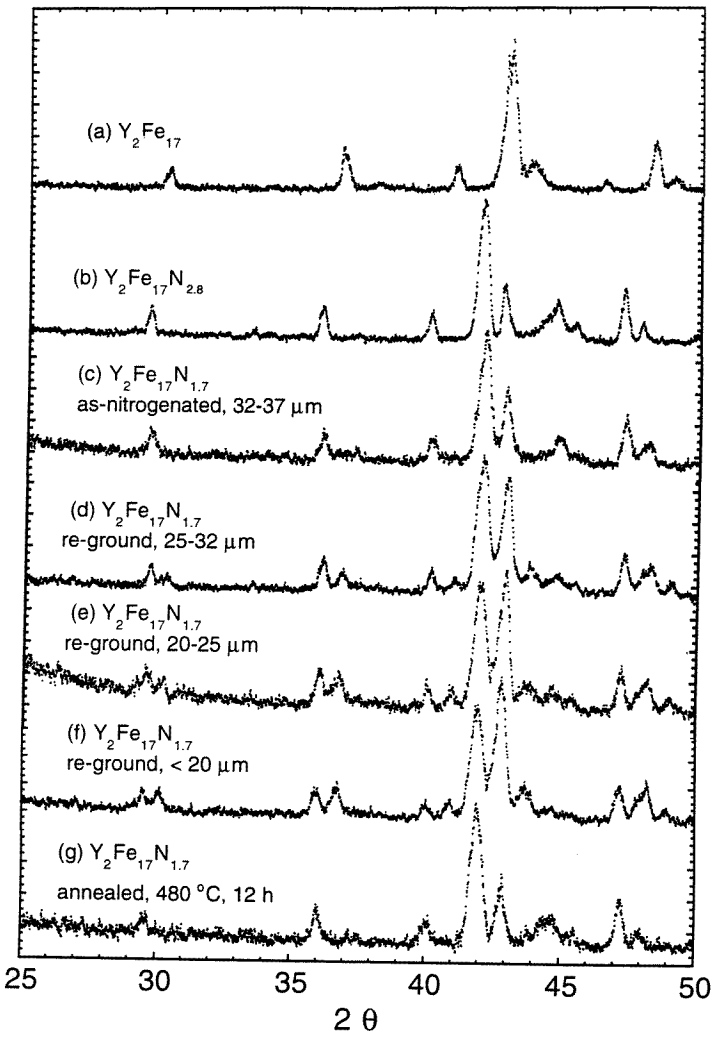

Figure 1. Cu Kα XRD patterns for Y_2Fe_{17} and its nitrides: (a) Y_2Fe_{17} parent compound; (b) $Y_2Fe_{17}N_{2.8}$ 'completely' nitrided; (c) $Y_2Fe_{17}N_{1.7}$ as nitrogenated, particle size 32–37 μm; (d) $Y_2Fe_{17}N_{1.7}$ re-ground, particle size 25–32 μm; (e) $Y_2Fe_{17}N_{1.7}$ re-ground, particle size 20–25 μm; (f) $Y_2Fe_{17}N_{1.7}$ re-ground, particle size <20 μm; (g) $Y_2Fe_{17}N_{1.7}$ vacuum annealed at 480 °C for 12 h.

stopped. Therefore, the N distribution present at the time when the oven was turned off was retained. The N content, namely the average number of N atoms per Y_2Fe_{17} formula unit, was determined by weighing each $Y_2Fe_{17}N_x$ sample before and after nitrogenation. Some nitrided samples were further annealed in vacuum using the same apparatus as that used for nitrogenation.

XRD was employed to obtain structural information concerning the phase constituents of the sample powders upon nitrogenation. Figure 1(a)–(f) shows the XRD patterns obtained from the parent Y_2Fe_{17} sample, the 'completely' nitrided sample ($Y_2Fe_{17}N_{2.8}$) and the $Y_2Fe_{17}N_{1.7}$ sample after various grinding treatments, respectively. An essentially single

hexagonal Y_2Fe_{17} phase with no bcc α-Fe present was identified for the parent sample (figure 1(a)). As shown in figure 1(b), in addition to a small amount of α-Fe which occurred in all of the nitrided samples, the completely nitrided sample, i.e., $Y_2Fe_{17}N_{2.8}$, has the same structure as the parent Y_2Fe_{17} sample, but all of the Bragg peaks are shifted to lower angles. For the intermediate-N-content sample $Y_2Fe_{17}N_{1.7}$, the XRD peaks shown in figure 1(c) are *not* located between those corresponding to the parent and the completely nitrided samples; instead, the locations of these Bragg peaks are essentially the same as that for $Y_2Fe_{17}N_{2.8}$. This result indicates that the nitrogen atoms are concentrated in the surface region. Otherwise, if they were distributed throughout the entire particle, one would observe smaller shifts of these XRD peaks. In order to examine the structure of the interior of the particle, the $Y_2Fe_{17}N_{1.7}$ sample powders were further re-ground step by step to the size ranges 32–35, 20–25 and <20 μm, and XRD experiments were carried out on the samples of each size range. Grinding the particles either removes their outer surface or breaks the particles into pieces, each of which allows the interiors of the particles to be exposed to x-rays. As shown in figure 1(d)–(f), each Bragg diffraction for the re-ground powders consists of two peaks: one corresponds to the parent Y_2Fe_{17} phase and the other to the completely nitrided phase. As the particle size is reduced, the peaks corresponding to the parent phase become stronger. The appearance of two XRD patterns for samples with intermediate N content is direct evidence for the existence of the nitrided–unnitrided configuration, and this study indicates that the nitrided region is predominantly in the surface region of the particle. Figure 1(g) shows the XRD pattern for the original $Y_2Fe_{17}N_{1.7}$ sample (32–37 μm) after vacuum annealing at 480 °C for 12 h. A comparison between figure 1(c) and 1(g) clearly shows that the vacuum annealing does not produce any change in the two-phase configuration. Therefore, it is evident that the N distribution formed in a nitrogenation process remains unchanged upon annealing.

N outgassing experiments were performed on several $Y_2Fe_{17}N_x$ samples using a temperature-programmed desorption apparatus [15]. A tube containing a $Y_2Fe_{17}N_x$ sample was subject to a flow of ultrapurified He gas at a fixed rate. The desorbed N atoms from the sample were mixed with the flowing He gas, which was analysed with TCD apparatus. Figure 2(a) shows the N desorption rate as a function of temperature obtained from the $Y_2Fe_{17}N_{2.8}$ sample. The first peak, at approximately 120 °C, corresponds to the outgassing of the N atoms absorbed at the particle surface. The second peak, at 380 °C, corresponds to the outgassing of N atoms from the interior of the particle. The huge increase in N release rate above 600 °C is due to a phase decomposition into YN and α-Fe. In addition, the experiment was repeated with the temperature scan programmed to stop rising at 460 °C. As shown in figure 2(b), the N effluence process takes less than 15 min at 460 °C. The N outgassing was also measured using a method similar to thermopiezic measurements for the same sample at 460 °C. It was estimated from these measurements that about 4–7 at.% of the inserted N atoms can be released by vacuum annealing, while most of the N atoms cannot be evacuated until the decomposition takes place (>600 °C). Similar results have been observed in other R_2Fe_{17} nitrides [16–18].

^{89}Y hyperfine field (HF) distribution measurements were carried out at 4.2 K using a phase-coherent spin-echo NMR spectrometer over a frequency range from 20 to 60 MHz. Figure 3 shows the ^{89}Y NMR spectra for $Y_2Fe_{17}N_x$ with $x = 0$, 0.3, 1.5, 2.0, 2.6 and 2.8. For the parent Y_2Fe_{17} sample, a single peak centred at 42.5 MHz was observed. For the nitrides, four resonance peaks centred at 42.7, 36.5, 29.3 and 26.5 MHz were observed, which are labelled Y(0), Y(1), Y(2) and Y(3), respectively. The Y nucleus carried a very small moment; the HF at a ^{89}Y nucleus is the so-called transferred hyperfine field (THF) which originates from the conduction electron polarization caused by the spins of the Fe 3d

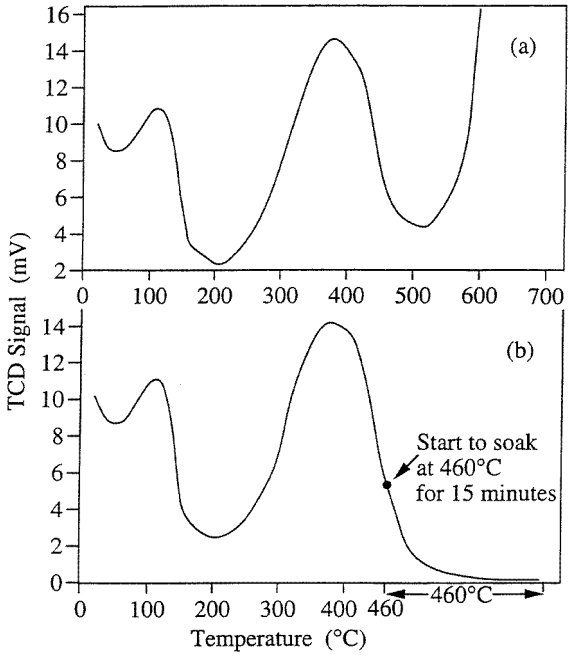

Figure 2. TCD of N outgassing for $Y_2Fe_{17}N_{2.8}$ as a function of temperature measured at a temperature-ramping rate of 15 K min^{-1}. (a) The temperature was raised to 600 °C when the decomposition occurred; (b) the temperature was raised to 460 °C and the sample was allowed to remain at 460 °C for 15 min.

electrons surrounding Y. For $Y_2Fe_{17}N_x$, the addition of an N atom into the 6c interstitial site surrounding a Y atom leads to a change in the electronic states of the Y atom. As a consequence, this results in a shift of the ^{89}Y NMR frequency, the magnitude of the shift being dependent on the number of N atoms surrounding the Y atom. Therefore, the peaks Y(0), Y(1), Y(2) and Y(3) are assigned to the Y atoms having 0, 1, 2 and 3 N atoms in the surrounding octahedral interstitial sites, respectively [19, 20]. Since ^{89}Y NMR spectra reflect the local environments surrounding Y atoms, any changes in Y–N configuration will lead to a variation in the ^{89}Y NMR spectrum. As shown in figure 3, the major change in the ^{89}Y NMR spectrum with increasing N content lies in the drastic decrease of the Y(0) peak intensity with respect to the Y(1), Y(2) and Y(3) peaks, which have a relatively constant intensity ratio. Very similar results were obtained for the $Y_2Fe_{17}N_x$ samples with rhombohedral crystal structure [6]. It is deduced based on the NMR spectra that the particle forms a two-phase (nitrided–unnitrided) configuration, and that Y(0) peak originates from Y atoms in the unnitrided region while the Y(1), Y(2) and Y(3) peaks originate from Y atoms in the nitrided region. In considering the NMR peak intensities for magnetically ordered materials, the effect of the NMR enhancement factor on the NMR spectrum has to be taken into account [21]. It was found in our experiments on these samples that the enhancement factors for Y(1), Y(2) and Y(3) peaks are approximately the same, but are different from that for the Y(0) peak. This makes it difficult to obtain the precise volume ratio of the nitrided region to the unnitrided region from comparing the areas under the Y(1), Y(2) and Y(3) peaks with that under the Y(0) peak, because it is difficult to obtain a precise value of the enhancement factor for each peak. However, the decrease of the

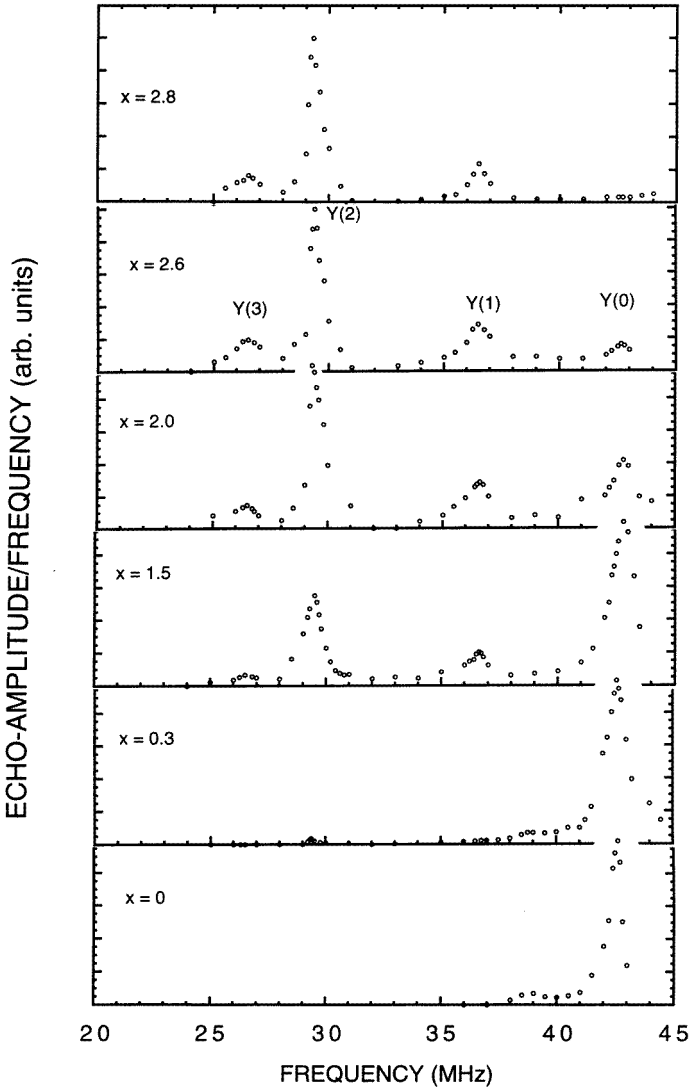

Figure 3. ^{89}Y spin-echo NMR spectra for $Y_2Fe_{17}N_x$ measured at 4.2 K.

Y(0) peak intensity and the lack of change of the relative intensities of the Y(1), Y(2) and Y(3) peaks upon nitrogenation clearly demonstrate that the nitrogenation process is the growth of the nitrided region while the N concentration, hence the Y–N configuration, in the nitrided region does not change with nitrogenation process. We refer the reader to [6] for a detailed discussion. The similarity of NMR spectra between the rhombohedral and hexagonal $Y_2Fe_{17}N_x$ samples indicates that the nitrided–unnitrided configuration formed in $Y_2Fe_{17}N_x$ is an intrinsic feature, and is not due to structural disordering or possible defects in these samples.

Figure 4(a) shows the ^{89}Y NMR spectrum for $Y_2Fe_{17}N_{1.7}$. The observed relative ^{89}Y NMR peak intensity ratio is Y(0):Y(1):Y(2):Y(3) = 0.62:0.07:0.27:0.04; while the calculated probability ratio for a homogeneous distribution of the N atoms in the particle

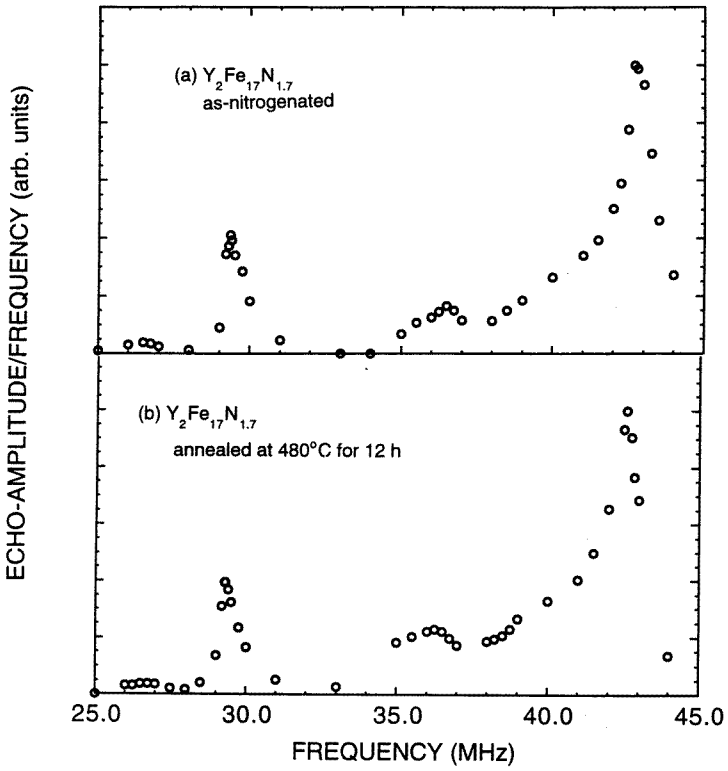

Figure 4. ^{89}Y spin-echo NMR spectra for $Y_2Fe_{17}N_{1.7}$ measured at 4.2 K: (a) for the as-nitrogenated sample; (b) for the same sample but annealed at 480 °C in vacuum for 12 h.

is 0.08:0.32:0.42:0.18 [6]. Such a large difference also implies that the absorbed N atoms are actually concentrated in the nitrided region. If the N atoms in the octahedral sites could migrate freely at the nitrogenation temperature, then in a vacuum annealing process at about the same temperature these N atoms would either leave the particle or diffuse further toward the interior of the particle to reach a homogeneous distribution in about the same period of time as that for nitrogenation. In the former case, we would have observed the disappearance of the Y(1), Y(2) and Y(3) peaks and a strong increase in the Y(0) peak intensity; in the latter case, we would have observed a significant change in the relative intensities of these four peaks. Figure 4(b) shows the ^{89}Y NMR spectra for the $Y_2Fe_{17}N_{1.7}$ sample after a vacuum annealing at 480 °C for 12 h. Comparison of figure 4(a) and 4(b) shows no change in the Y–N configuration upon annealing, indicating a good stability of N distribution in the octahedral interstitial sites at the nitrogenation temperature.

3. Discussion

3.1. Immobilization of nitrogen atoms which enter the octahedral interstitial sites

One possibility for the irreversibility of N uptake in the 2:17 phase is a large surface barrier or a large binding energy of $R_2Fe_{17}N_x$, compared with that for N_2. If these were the case, a heat treatment would cause the N atoms to relocate and ultimately reach a homogeneous

distribution. XRD would show a single-phase pattern with intermediate lattice parameters, and the ^{89}Y NMR spectrum would have a significant change. The results shows in figures 1 and 3 have ruled out this possibility. Furthermore, the fact that some fraction of the absorbed N atoms can be evacuated from the sample (figure 2) implies that the surface barrier is not prohibitively large and the desorption is not forbidden. In exploring the intrinsic reason responsible for the observed features, the following two interactions should be considered [14, 22]. (i) *N–N interaction*. If the octahedral-site N atoms are mobile, an elastic N–N coupling may keep them densely distributed in a (nitrided region). (ii) *N–lattice interaction*. If the N atoms which enter the octahedral sites are trapped at these sites due to a strong N–lattice bonding, then a nitrided region can be formed and these N atoms are no longer mobile.

The insertion of a gas atom into an interstitial site creates a long-range strain field, which may affect the accommodation of subsequent atoms. When the total elastic energy involved for two gas atoms that are located close to each other is smaller than when they are far apart, the coupling is equivalent to an attractive interaction [23] under which the gas atoms may be densely distributed or form a gas-atom-rich phase. On the other hand, thermal energy tends to cause the gas atoms to distribute randomly. Therefore, there is a critical temperature, T_c, below which the interatomic coupling dominates and favours a gas-atom-rich distribution; while above T_c the gas atoms have a random distribution. The larger the elastic energy caused by the insertion, the higher T_c. The conditions for this mechanism are rather severe: the gas-phase insertion temperature should be significantly lower than T_c while the inserted gas atoms should be highly mobile at that temperature. In some metal–hydrogen systems, such as Nb–H, V–H and Pd–H, H atoms are mobile at temperatures even below room temperature and the H addition produces about 20% volume expansion of the host lattice [24]. As a consequence, hydrogen-rich phases are formed with critical temperatures of about 300 °C [25, 26]. With regard to metal–nitrogen systems, to our knowledge, a case has never been observed in which the N–N coupling causes a similar phenomenon. As for 2:17 nitrides, if an N–N interaction were the major cause for the observed nitrided–unnitrided configuration in the Y_2Fe_{17} lattice, then the N–N coupling would be strong enough to establish a critical temperature significantly greater than 480 °C. However, by comparing the volume expansion produced by N insertion into R_2Fe_{17} (about 7%) with that produced by H insertion into Nb or Pd metals (about 20%), one expects the critical temperature for 2:17 nitrides to be below room temperature. Therefore, the indirect N–N interaction does not appear to be a factor in determining the observed N distribution in the 2:17 lattice.

The facts that most of the N atoms cannot be removed from the Y_2Fe_{17} lattice and, especially, that the octahedral-site N atoms cannot be relocated at 480 °C, indicate that the octahedral-site N atoms are actually immobilized. The TCD and NMR experiments reveal that there are two types of N atom in Y_2Fe_{17} nitrides: the immobile N atoms, which are located in the octahedral sites, and mobile N atoms, which are located at other sites, such as the tetrahedral interstitial sites as proposed previously [27, 28]. Each individual N atom is mobile at first and diffuses for a certain period of time and then, when it occupies an octahedral interstitial site, is immobilized. The immobilization leads to a complete accommodation of N atoms for the octahedral interstitial sites in the outer region of the particle, instead of a continuous solid solution distribution. The subsequent (mobile) N atoms migrate a longer distance before encountering an empty octahedral site, this continuing the nitrogenation process. Such a large change in diffusion behaviour for N atoms before and after entering the octahedral sites is due to an N–lattice chemical bonding effect. The measured value of the diffusion activation energy, E_a, for the mobile N atoms in the 2:17

lattice is about 0.9 eV [4], which is similar to the activation energy for N diffusion in metals. At 400 °C (a typical nitrogenation temperature for Sm_2Fe_{17}), $\exp(-E_a/k_BT) = 1.8 \times 10^{-7}$. Assuming that the site binding at the octahedral site leads to a 50% increase in E_a, then $\exp(-E_a/k_BT) = 8.0 \times 10^{-11}$. This means that if a weakly bonded N atom takes about 10 h to migrate a given distance, then for a rather strongly bonded N atom the same process takes several years, i.e., it is actually immobilized.

The diffusion activation energy is intimately related to the size of the interstitial site. Perhaps the immobilization of N atoms in the octahedral interstitial sites that we observe in the Y_2Fe_{17} nitrides is an extreme case since Y_2Fe_{17} has small lattice parameters compared with other 2:17 compounds. It is possible that the octahedral-site N atoms in some 2:17 compounds are still mobile but with a smaller diffusion constant. No matter whether or not the octahedral-site N atoms are immobilized, the existence of two types of N atom with different diffusivities is very likely to be the case for all of the 2:17 systems and should be taken into account in theoretical treatment of the N diffusion in these systems.

The effects of site binding on the diffusion behaviour of gas atoms with different diffusivities have been dealt with in many articles [29]. However, in the study of 2:17 nitrides, the importance of the N-lattice interaction in the diffusion process has not been realized up to date. In order to show how a trapping effect may drastically affect a gas atom diffusion process and how the N–lattice interaction may cause the observed features in 2:17 nitrides, we modify the diffusion equation to a lattice containing different interstitial sites corresponding to different diffusivities, and then apply the calculated results to understand the nitrogenation in the 2:17 lattice (for a brief discussion, see [14]).

3.2. Diffusion of gas atoms in a lattice containing two types of interstitial site

Consider a spherical particle of radius R surrounded by a gas phase of atoms (such as N_2 or C). In the particle, there are two different (f and t) types of interstitial site which can accommodate the gas atoms, and the gas atoms in the two types of site are referred to as f- and t-type atoms, respectively. The f-type (*free*) atoms are weakly bonded with the lattice and can migrate freely; the t-type (*trapped*) atoms are subjected to a stronger attractive interaction with the lattice. It is assumed that both the f- and t-type atoms are all diffusive; however, the t-type atoms have a smaller diffusion constant than the f-type atoms. Let $c_f(r, t)$ and $c_t(r, t)$ be the concentrations of the f- and t-type gas atoms, respectively, at a distance r from the centre of the particle and at a time t. $c_{f0} = c_f(R, t)$ and $c_{t0} = c_t(R, t)$ are the corresponding concentrations at the surface of the particle. Also, these are the equilibrium values for $c_f(r, t)$ and $c_t(r, t)$ as $t \to \infty$ and $c_{f0} + c_{t0}$ is the total gas atom concentration at equilibrium state. We assume $c_{f0} \leqslant c_{t0}$. In addition to the migration of both types of N atom, there can also exist an exchange between f and t types for individual atoms. Because of a lower diffusivity for the t-type atoms, the probability for a gas atom to change from f to t type is greater than that from t to f type, and, thus, one observes only a transfer of gas atoms from f-type to t-type sites. The modified diffusion equations for the two types of atom in the particle can be written as

$$\boldsymbol{J}_f(r, t) = -D_f \boldsymbol{\nabla} c_f(r, t) \tag{2}$$

$$\partial c_f(r, t)/\partial t = -\boldsymbol{\nabla} \cdot \boldsymbol{J}_f(r, t) - \partial c_{ft}(r, t)/\partial t \tag{3}$$

$$\boldsymbol{J}_t(r, t) = -D_t \boldsymbol{\nabla} c_t(r, t) \tag{4}$$

$$\partial c_t(r, t)/\partial t = -\boldsymbol{\nabla} \cdot \boldsymbol{J}_t(r, t) + \partial c_{ft}(r, t)/\partial t \tag{5}$$

where $\boldsymbol{J}_f(r, t)$ and $\boldsymbol{J}_t(r, t)$ are the radial atomic current fluxes across a unit area for the f- and t-type gas atoms, respectively. D_f and D_t are the corresponding diffusion constants.

The term $\partial c_{ft}(r,\ t)/\partial t$ in (3) and (5) represents the rate for the gas atoms changing from f to t type. Due to atomic transfer between the two types of site, the fast-migrating (f-type) atoms fill the t-type sites, resulting in the occupancy of the t-type sites near the surface of a particle to the equilibrium concentration c_{t0}. This makes a gas atom distribution deviate from the CSSD pattern. Figure 5(a) illustrates a typical distribution profile. The particle can be separated into three regions. In region I (ideally this is the outer shell of the particle with a radial thickness of $R-R_0$), the t-type sites have been filled to its equilibrium concentration c_{t0} for $R_0 \leqslant r \leqslant R$. We note that R_0 is time dependent as shown in figure 5(a). The filling of the f-type sites in this region follows a pattern characteristic of free diffusion:

$$\boldsymbol{J}_t(r,\ t) = 0 \qquad \partial c_t(r,\ t)/\partial t = 0 \qquad \partial c_{ft}(r,\ t)/\partial t = 0 \tag{6}$$

and

$$\partial c_f(r,\ t)/\partial t = D_f \boldsymbol{\nabla}^2 c_f(r,\ t) \qquad \text{for } R_0 \leqslant r \leqslant R. \tag{7}$$

In our previous work [14], the distribution of the f-type atoms from R to R_0 was obtained by taking the shell as an equivalent sphere. An alternative approach to obtain $c_f(r,\ t)$ is to solve the diffusion equation for a hollow spherical shell. The solution for this case is [30]

$$c(r,\ t) = c_{t0} + c_f(r,\ t) = c_{t0} + \frac{c_{f0}R(r-R_0) + c_f(R_0)R_0(R-r)}{r(R-R_0)} + \frac{2}{\pi r}\sum_{m=1}^{\infty} \frac{c_{f0}R\cos m\pi - c_f(R_0)R_0}{m} \sin\frac{m\pi(r-R_0)}{(R-R_0)} \mathrm{e}^{-m^2\pi^2 D_f t/(R-R_0)^2} \tag{8}$$

where $c(r,\ t) = c_f(r,\ t) + c_t(r,\ t)$ is the total gas atomic concentration, and $c_f(R_0)$ is the f-type gas concentration at R_0 ($c_f(R_0) \ll c_{f0}$). The total gas atom concentration at the boundary is $c_0(R_0) = c_{t0} + c_f(R_0) \simeq c_{t0}$..

Region II is a transition region in which the filling of both types of site is developing. (2)–(5) can be written as

$$\partial c_f(r,\ t)/\partial t + \partial c_t(r,\ t)/\partial t = D_f \boldsymbol{\nabla}^2 c_f(r,\ t) + D_t \boldsymbol{\nabla}^2 c_t(r,\ t) \qquad \text{for } R_0 \leqslant r \leqslant 0. \tag{9}$$

Here we introduce a parameter

$$k = c_t(r,\ t)/c_f(r,\ t). \tag{10}$$

k reflects the strength of gas–lattice interaction in t-type sites compared with that in the f type. In the extreme case where the t-type atoms are also weakly bonded with the lattice, i.e., $D_t \to D_f$, there is no gas atom transfer between the f- and t-type sites and k is equal to the ratio of the equilibrium concentrations for the two types of atom,

$$k \to k_0 = c_{t0}/c_{f0}. \tag{11}$$

With the existence of a gas–lattice interaction, the change in $c_t(r,\ t)$ in region II is caused by both the migration of t-type atoms and the transfer of gas atoms from f to t type. A greater trapping effect for the t-type sites corresponds to a larger $\partial c_{ft}(r,\ t)/\partial t$, which leads to more occupancy for the t-type sites than for the f-type sites. As a consequence, a larger value of k (than k_0) is reached. In the region where the t-type sites are not fully occupied and $k \gg k_0$, $c_t(r,\ t)$ results mainly from the transfer of gas atoms and is approximately proportional to $c_f(r,\ t)$, k can be approximately treated as a constant [14, 29] and, hence, (9) can be written as

$$\partial c_t(r,\ t)/\partial t = D\boldsymbol{\nabla}^2 c_t(r,\ t) \qquad D = \big(D_t k + D_f\big)\big/(1+k) \tag{12}$$

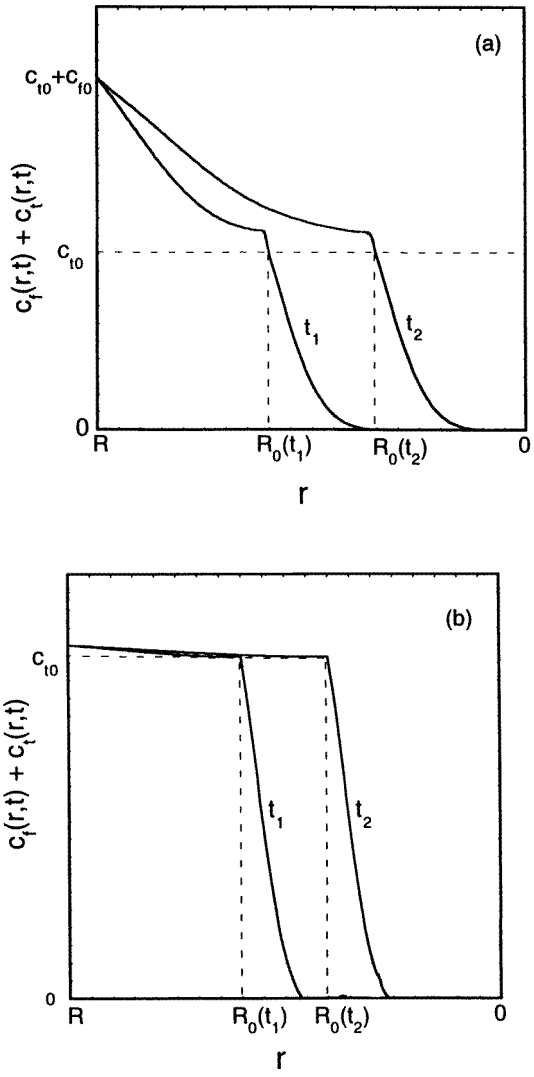

Figure 5. (a) An illustration of radial distribution profiles for gas atom concentration, $c(r, t) = c_f(r, t) + c_t(r, t)$, at different times. (b) An illustration of N distribution profiles at different nitrogenation times for 2:17 nitrides for which $c_{t0} \gg c_{f0}$ and $D_t \to 0$.

where D is the 'effective' diffusion constant. The same equation is also obtained for the f-type atoms. The solution of (12) is

$$c(r,\, t) = c_0\big(R_0\big)\left[1 - \frac{2R_0}{\pi r}\sum_{m=1}^{\infty}\frac{(-1)^{m+1}}{m}\sin\frac{m\pi r}{R}\mathrm{e}^{-m^2\pi^2 Dt/R_0^2}\right]. \tag{13}$$

A significant feature of the trapping diffusion model is that there is a region (region III) in which there are essentially no gas atoms:

$$c(r,\, t) \simeq 0. \tag{14}$$

The major difference between (7) and (12) lies in the different diffusion constants appearing in the exponential arguments. Because $D < D_f$, a larger concentration gradient is expected in region II than in region I. Thus, a steplike gas atom distribution is formed. Figure 5(a) shows the gas atom distribution profiles at two different times. With increasing time, while keeping the gas supply constant, R_0 moves toward the interior of the particle. The diffusion process ends with the equilibrium gas atom concentration $c_0 = c_{t0} + c_{f0}$ throughout the particle. Although (8) and (13) are only an approximate description (especially for $r \to R_0$) of gas atom distribution, the pattern shown in figure 5(a) is a fundamental feature of the trapping diffusion process.

Extending the above general discussion to the N diffusion process in the 2:17 lattice, the t- and f-type atoms denote the octahedral- and non-octahedral-site N atoms, respectively, and D_t and D_f denote the diffusivities for the N atoms in these two types of site. Under most often employed nitrogenation conditions with about 1 bar N_2 pressure, the N insertion into R_2Fe_{17} is a typical example of the trapping diffusion process: $D_t \ll D_f$ (or even $D_t \to 0$), and $c_{t0} \gg c_{f0}$. In this case, the distribution of the f-type N atoms reaches its steady state for each stage, and (8) becomes

$$c(r,\, t) = c_{t0} + c_f(r,\, t) = c_{t0} + \left[c_{f0}R\left(r - R_0\right) + c_f\left(R_0\right)R_0(R - r)\right]\Big/ r\left(R - R_0\right). \tag{15}$$

With a very small concentration for mobile N atoms, the nitrogen distribution profile in region I is essentially flat and the transition region is very sharp. Figure 5(b) illustrates the N distribution profile. A detailed discussion of the time dependence of R_0 has been carried out by Yang *et al* [31]. Such a sharp transition has been observed in $Y_2Fe_{17}N_x$ [6], $Nd_2Fe_{17}N_x$ [5, 7], $Dy_2Fe_{17}N_x$ [9] and $Sm_2Fe_{17}N_x$ [33]. The condition $D_t \to 0$ corresponds to a chemical reaction diffusion process under which the (t-type) diffusant is trapped to produce a new compound, or is immobilized.

The difference between the free diffusion and trapping diffusion models lies in that the free diffusion model assumes one type of N atom with the same diffusion constant while the trapping diffusion model considers the existence of two types of N atom with different diffusion constants. Diffusivity is determined by the diffusion activation energy relative to thermal energy. When the difference in activation energy for these two types of N atom is large compared with thermal energy, the system has to be described by the trapping diffusion model. Especially, when the migration for t-type atoms is very slow compared with that for f-type N atoms, these atoms can be treated as immobile within the observation period of time. On the other hand, if the difference in activation energy is negligibly small compared with the thermal energy, then $D_t \to D_f$, $k \to k_0$ and (2)–(5) reduce to the classical diffusion equation [32]. Therefore, the free diffusion model [10, 11] is the high-temperature approximation of the trapping diffusion model [14]. For each 2:17 system, depending on the temperature, N diffusion can be a trapping diffusion or a free diffusion process. Taking Sm_2Fe_{17} as an example, XRD, TEM and magnetization experiments reveal that nitrogenation at temperatures below 450 °C results in a nitrided–unnitrided configuration [12, 33, 34], typical for the trapping diffusion process, while the XRD pattern obtained from samples nitrided at 575 °C supports the free diffusion model [10]. In order to avoid phase decomposition, nitrogenation for R_2Fe_{17} is performed below 500 °C, for which case the nitrogen diffusion is characteristic of trapping diffusion.

3.3. Measurement of the diffusion frequency factor D_0

It was found in nitrogenation experiments of 2:17 systems that the measured value of E_a was similar to that for N diffusion in metals [4]. In principle, the value of D_0 for N diffusion

in the 2:17 lattice should be similar to that for N diffusion in metals. However, experiments provided somewhat complicated results: the magnitude of D_0 deduced by fitting the very early stage of nitrogen uptake (within 15 min [10]) is similar to the expected value for N diffusion in metals (1 $mm^2\ s^{-1}$), while the magnitude of D_0 deduced by fitting the entire nitrogenation process (which normally lasts longer than 10 h) is about four orders of magnitude smaller [4], which seems 'unreasonable'. Since N diffusion in the early stage may be significantly influenced by defects of cracks, results obtained from the prolonged nitrogenation process are more reliable in describing the bulk diffusion behaviour. Such a small apparent frequency factor can be understood in the framework of the trapping diffusion model. The evolution of nitrogenation is through the occupation of the octahedral interstitial sites in region II. According to (12), what is obtained by monitoring the N absorption process is the effective diffusion constant,

$$D \simeq D_f/(1+k) = \left[D_{f0}/(1+k)\right]\mathrm{e}^{-E_{af}/k_BT} \tag{16}$$

where E_{af} is the diffusion activation energy for the f-type N atoms. Thus, what is deduced from the D versus T curve is an apparent frequency factor $D_{f0}/(1+k)$, which is much smaller than D_{f0}. As to the activation energy, as shown in (16), the value deduced from the D versus T curve is the activation energy for the f-type N atoms.

The difference between the apparent diffusion frequency factor and D_0 provides information concerning the strength of the trapping effect. For N in Sm_2Fe_{17}, it is estimated from the experiments that $k \sim 10^3$–10^4. The outgassing experiments show that a few per cent of the absorbed N atoms are f type, i.e., $k_0 \sim 10^1$–10^2. This implies $k \sim 10^2$–$10^3 k_0$, indicating that the N–lattice bonding at the octahedral sites is indeed strong. At this point, one expects a good stability of N distribution in the 2:17 lattice.

3.4. Consideration of the nitrogenation conditions

Since the nitrogenation develops mainly through the migration of the f-type N atoms, the nitrogenation temperature for a given system should be set such that the f-type N atoms in the system have a satisfactory diffusivity D_f ($\sim \mathrm{e}^{-E_{af}/k_BT}$) so as to complete the nitrogenation process within a reasonable period of time. Since E_{af} varies from system to system, the nitrogenation temperature may be adjusted correspondingly. For instance, for Sm_2Fe_{17} the nitrogenation can be conducted at 350 °C while for Y_2Fe_{17} the temperature should be higher than 450 °C. Depending on the parent compounds, the octahedral-site N atoms can be either mobile or immobilized at a given nitrogenation temperature. In the case where the octahedral-site N atoms are immobilized, the nitrogenation process forms a steplike N distribution profile with a sharp transition region. With all of the allowable octahedral sites being occupied, the N content in the nitrided region is the maximum, and the nitrogenation process ends with a full occupancy of all of the allowable octahedral interstitial sites. The ambient gas pressure and temperature determine c_{f0} and D_f and, hence, vary the N uptake rate, but these conditions play a very limited role in affecting the N content in the fully nitrided region. Also, the immobilization of the N atoms causes the observed irreversibility for the N uptake. There may exist some cases where the octahedral-site N atoms are not immobilized: (i) when nitriding 2:17 compounds which have larger lattice parameters, and, hence, smaller activation energies, (ii) when nitriding together with hydrogenation for which the expanded lattice due to H insertion may reduce the activation energy, and (iii) when nitriding $R_2Fe_{17-x}M_x$ where the substitution of an element M, such as Ga or Al, for Fe may lead to larger lattice parameters [35]. In the case where the octahedral-site N atoms are mobile but with smaller diffusivity, D_t ($\sim \mathrm{e}^{-E_{at}/k_BT}$, where E_{at} is the diffusion energy

for the octahedral-site N atoms), than that for f-type N atoms, the nitrogenation process also forms a steplike N distribution profile but with a broader transition region. In this case, not all of the allowable octahedral sites are occupied by N atoms: instead, the N content in the nitrided region is dependent on the nitrogenation conditions, and the nitrogenation process ends with a smaller N occupancy. By adjusting the N_2 pressure and temperature, the equilibrium N content can be controlled almost throughout the entire range from zero to nearly the maximum. In this case, the N uptake may be reversible, i.e., the octahedral-site N atoms can be evacuated by vacuum annealing. Since the evacuation process is through the migration of the octahedral-site N atoms, it takes a much longer time than the nitrogenation. In order to insert a larger number of N atoms into the 2:17 lattice, the nitrogenation temperature should be chosen such that the f-type N atoms can migrate with a significant diffusion rate while the octahedral-site N atoms are almost immobile.

N distribution homogeneity is important for good permanent magnet performance. When there are unnitrided regions with sizes greater than the so-called exchange-coupling length [36, 37], which is less than 10 nm for R_2Fe_{17} nitrides, the magnetic properties in these regions will remain soft and, as a consequence, the permanent magnetic properties of the material might be poor. This effect has been observed in the study of Sm_2Fe_{17} nitrides [34]. For some 2:17 systems, it is possible to anneal the partially nitrided sample to obtain a homogeneous $R_2Fe_{17}N_x$ with intermediate N content at temperatures below 500 °C. Homogenizing is through the migration of the octahedral-site N atoms; the homogenizing process is determined by D_t. Since $E_{at} > E_{af}$, a higher annealing temperature may be required so as to make the octahedral-site N atoms mobile; also, the process may take a much longer period of time than needed for nitrogenation. It was observed in the study of $Sm_2Fe_{17}N_x$ [13] that lattice parameters for the as-prepared samples with intermediate N content are very close to those for the completely nitrided sample, indicating the formation of an almost fully nitrided region in the surface of the particle; while after a long time annealing homogeneous N distributions are reached in these samples and, hence, the lattice parameters reduce to intermediate values. These results provide evidence of the trapping diffusion process of N in the Sm_2Fe_{17} lattice. In addition to the phase decomposition, annealing at a higher temperature may cause a release of N atoms from the lattice if there is no means to prevent N outgassing.

The exploration of phase decomposition of 2:17 compounds during a nitrogenation process is one of the most important tasks. The facts that $Sm_2Fe_{17-x}Si_xC_y$ ($y \leqslant 2.7$) [38] and $Sm_2Fe_{17-x}Ga_xC_y$ ($y \leqslant 1.5$) [35] are stable beyond 700 °C reveal a possibility of stabilizing the 2:17 phase and, perhaps, of easing the processing for $Sm_2Fe_{17}N_x$-based permanent magnets. In addition, it is not certain whether the decomposition exists mainly in the surface region of the particle [10] or takes place in the boundary between the nitrided and unnitrided regions, where large stress and strain occur, and hence exists throughout the whole particle [6]. Further study of the details of the phase decomposition mechanism is greatly needed.

4. Conclusions

In order to study nitrogen diffusion in the 2:17 lattice, a combination of ^{89}Y spin-echo nuclear magnetic resonance, x-ray diffraction and thermoconductivity (outgassing) experiments has been carried out on $Y_2Fe_{17}N_x$ ($0 < x < 2.8$) samples. The results presented here, along with other experimental work, indicate that the octahedral-site N atoms are actually immobilized and only a small number of N atoms are free to migrate. Based on the experimental results, we have extended the diffusion formalism to a lattice

containing two types of site. The gas atoms in the two types of site are designed as 'trapped' type and 'free' type atoms. The former are subjected to a strong attractive interaction with the lattice and possess a relatively small diffusion constant; the latter are weakly bonded with the lattice and possess a large diffusion constant. The calculation shows that the accommodation of N atoms in these sites with vastly different diffusion constants, along with the transfer of N atoms between these sites, results in a steplike N distribution and an abnormally small (apparent) diffusion frequency factor. The experiments and theoretical analysis have proved that it is the N–lattice interaction, instead of N–N interaction, that traps the N atoms at the octahedral interstitial sites, resulting in the observed two-phase configuration, N uptake irreversibility and stability. It turns out that the N diffusion in the R_2Fe_{17} lattice is more like a chemical reaction diffusion process.

The goal of investigating N diffusion in the R_2Fe_{17} phase is to optimize the nitrogenation conditions for the largest improvement of the magnetic properties along with the smallest phase decomposition. In this regard, it is advantageous to insert N atoms in a previously expanded or stabilized 2:17 lattice at a relatively low temperature.

Acknowledgment

This work is supported in part by NSF grant DMR9319367 and the Connecticut Advanced Center for Manufacturing. The authors would like to thank P Panissod for many useful discussions.

References

[1] Buschow K H J 1991 *Rep. Prog. Phys.* **54** 1123
[2] Coey J M D and Sun H 1990 *J. Magn. Magn. Mater.* **87** L251
[3] Buschow K H J, Coehoorn R, de Waard D B and Jacobs T H 1990 *J. Magn. Magn. Mater.* **92** L35
[4] Coey J M D, Lawler J F, Sun H and Allan J E M 1991 *J. Appl. Phys.* **69** 3007
[5] Isnard O, Soubeyroux J L, Miraglia S, Furchart D, Garcia L M and Bartolome J 1992 *Physica* B **180/181** 624
[6] Zhang Y D, Budnick J I, Hines W A, Yang D P, Fernando W G, Xiao T D and Manzur T 1995 *Phys. Rev.* B **51** 12 091
[7] Colucci C C, Gama S, Ribeiro C A and Cardoso L P 1994 *J. Appl. Phys.* **75** 6003
[8] Persiano A I C, Ardisson J D, Batista F A, Colucci C C and Gama S 1994 *J. Magn. Magn. Mater.* **136** 149
[9] Girt Er, Altounian Z, Chen X, Mao M, Ryan D H, Sutton M and Cadogan J M 1994 *J. Appl. Phys.* **76** 6038
[10] Skomski R and Coey J M D 1993 *J. Appl. Phys.* **73** 7602
[11] Coey J M D, Skomski R and Wirth S 1992 *IEEE Trans. Magn.* **MAG-28** 2332
[12] Muller K-H, Cao Lei, Dempsey N M and Wendhausen P A P 1996 *J. Appl. Phys.* **79** 5045
[13] Brennan S, Skomski R, Qi Q and Coey J M D 1995 *J. Magn. Magn. Mater.* **140–144** 999
[14] Zhang Y D, Budnick J I, Hines W A and Yang D P 1995 *Appl. Phys. Lett.* **67** 208
[15] Xu W Q, Suib S L and O'Young C L 1993 *J. Catal.* **144** 285
[16] Kou X C, Grossinger R, Katter M, Wecker J, Schultz L, Jacobs H T and Buschow K H J 1991 *J. Appl. Phys.* **70** 2272
[17] Katter M, Wecker J, Kuhrt C, Schultz L and Grossinger R 1992 *J. Magn. Magn. Mater.* **117** 419
[18] Chen X, Altounian Z and Ryan D H 1993 *J. Magn. Magn. Mater.* **125** 169
[19] Kapusta Cz, Rosenberg M, Zukrowski J, Figiel H, Jacobs T H and Buschow K H J 1991 *J. Less-Common Met.* **171** 101
[20] Kapusta Cz, Rosenberg M, Erdmann K and Buschow K H J 1990 *Solid State Commun.* **76** 121
[21] See, e.g., Kiliptari I G 1995 *Phys. Rev.* B **52** 7346 and references therein
[22] Fujii H and Sun H 1995 *Handbook of Magnetic Materials* vol 9, ed K H J Buschow (New York: Elsevier) p 303
[23] Alefeld G 1972 *Ber. Bunsenges. Phys. Chem.* **76** 746
[24] Peisl H 1978 *Hydrogen in Metals* vol 1, ed G Alefeld and J Volkl (Berlin: Springer) p 53

[25] Fast J D 1965 *Interaction of Metals and Gases* (New York: Academic) p 183
[26] Flanagan T B and Oates W A 1988 *Hydrogen in Intermetallic Compounds* vol 1, ed L Schlapbach (Berlin: Springer) p 49
[27] Christodoulou C N and Komada N 1994 *J. Alloys Compounds* **206** 1
[28] Christodoulou C N and Komada N 1994 *J. Appl. Phys.* **76** 6041
[29] Crank J 1979 *The Mathematics of Diffusion* (New York: Oxford University Press) pp 286; 326
[30] Barrer R M 1944 *Phil. Mag.* **35** 802
[31] Yang D P, Zhang Y D, Budnick J I and Hines W A 1997 *J. Appl. Phys.* at press
[32] Crank J 1979 *The Mathematics of Diffusion* (New York: Oxford University Press) p 91
[33] Edgley D S, Saje B, Platts A E and Harris I R 1994 *J. Magn. Magn. Mater.* **138** 6
[34] Shen N X, Zhang Y D, Budnick J I and Hines W A 1996 *J. Magn. Magn. Mater.* **162** 265
[35] Shen B G, Wang F W, Kong L S, Cao L and Guo H Q 1993 *J. Magn. Magn. Mater.* **127** L267
[36] Kneller E F and Hawig R 1991 *IEEE Trans. Magn.* **MAG-27** 3588
[37] Schrefl T, Fischer R, Fidler J and Kronmuller H 1994 *J. Appl. Phys.* **76** 7053
[38] Li Z W, Zhou X Z and Morrish A H 1994 *J. Phys.: Condens. Matter* **6** L283